CSCE 2022 Annual Conference
Whistler, British Columbia
May 25th – 28th, 2022

RELIABILITY ASSESSMENT OF CONCRETE-FILLED RHS BEAM-COLUMN DESIGN PROVISIONS

Rahbarimanesh, Fatemeh[1], and Tousignant, Kyle[1,2]
[1]Dalhousie University, Canada
[2]kyle.tousignant@dal.ca

Abstract: Revisions were recently proposed to the way in which concrete-filled hollow structural section members are handled in CSA S16. These revisions were based on previous research, comparisons to experiments, and an approximate first-order reliability method analysis of the new and existing provisions. Herein, this topic is further expanded by using Monte Carlo Simulations (MCS) to evaluate the reliability of design rules for concrete-filled rectangular hollow section (RHS) beam-columns. A representative set of 10 concrete-filled RHS members is analyzed with variations in wall slenderness, effective length, and loading eccentricity. Using MCS, reliability indices (β^+) are determined over a range of live-to-dead load ratios. The β^+ values are compared to the code-specified target of $\beta^+ = 3.0$ in Annex B of CSA S16.

1 INTRODUCTION

Over the last two decades, American and European design provisions for concrete-filled hollow structural sections (HSS) under static loading (in AISC 360 and Eurocode 4, respectively) have evolved to permit the use of larger tube sizes, slenderer cross-sections, and longitudinal steel reinforcing bars. In contrast, the design provisions in Canada for concrete-filled HSS (in CSA S16 Clause 18.2) (CSA 2019a) have remained relatively constant and limited in scope.

Recently, following the completion of CIDECT Design Guide No. 4, 2nd edition (on concrete-filled HSS under static, impact, blast, seismic and fire loading) (Zhao et al., 2019), Tousignant and Packer (2022a,b) conducted a review of the design rules in CSA S16 Clause 18.2 (CSA 2019a), which led to proposed changes in its scope (i.e., material and cross-section classification limitations) and several provisions (i.e., for compressive resistance, flexural resistance, and beam-columns). An overview of these proposed changes is given in Tousignant and Packer (2022c).

The proposed changes by Tousignant and Packer (2022a,b) to the CSA S16 design formulae for the compressive resistance and bending resistance of concrete-filled HSS were supported, in part, by approximate first-order reliability method analyses that utilized data from over 450 tests to determine their inherent safety indices over a range of design scenarios (Tousignant and Packer 2022a,b); however, the impact of these proposed changes on the reliability of the beam-column interaction equation(s) (in Clause 18.2.4) was not directly assessed.

In this paper, Monte Carlo simulations (MCS) are used to extend the above work by re-analyzing data from Tousignant and Packer (2022a,b) and the corresponding database (Thai et al. 2019) to determine inherent

reliability indices (β^+) for the concrete-filled rectangular hollow section (RHS) beam-column design provisions proposed by Tousignant and Packer (2022b). Section 2 presents an overview of the current rules and the proposal; Sections 3 to 5 discuss the MCS approach; and Section 5.2 summarizes the results. The conclusions of this research study are presented in Section 6.

2 DESIGN PROVISIONS FOR CONCRETE-FILLED RHS BEAM-COLUMNS

2.1 CSA S16:19

The current design rules for concrete-filled RHS beam-columns (in CSA S16:19 Clause 18.2.4) apply to members with 20 MPa ≤ concrete strength (f_c') ≤ 40 MPa, and sections with flat width-to-thickness ratios (b_{el}/t) that meet the limits in Table 1. These limits are intended to ensure that the RHS can undergo complete plastification.

Table 1: Limits for concrete-filled RHS elements in axial or flexural compression

Action	Element	Limit(s)	
		CSA S16:19	Proposed
Axial compression	Flanges	$1{,}350/\sqrt{F_y}$	$1{,}350/\sqrt{F_y}$
	Webs	$1{,}350/\sqrt{F_y}$	$1{,}350/\sqrt{F_y}$
Flexural compression	Flanges	$1{,}350/\sqrt{F_y}$	$1{,}010/\sqrt{F_y}$
	Webs	$1{,}350/\sqrt{F_y}$	$1{,}340/\sqrt{F_y}$

Provided that these limits are met, concrete-filled RHS beam-columns can be proportioned according to Eq. [1]:

$$[1]\quad \frac{C_f}{C_{rc}} + \frac{\beta\omega_1 M_f}{M_{rc}\left(1-\frac{C_f}{C_{ec}}\right)} \le 1.0 \quad \text{and} \quad \frac{M_f}{M_{rc}} \le 1.0$$

where C_f = factored compressive force; M_f = factored moment; C_{rc} = compressive resistance; M_{rc} = moment resistance; ω_1 = coefficient to determine the equivalent uniform bending effect (found in CSA S16:19 Clause 13.8.6); C_{ec} = Euler buckling strength; and β = coefficient for bending.

In Eq. [1], C_{rc} is taken as:

$$[2]\quad C_{rc} = \frac{\tau\phi A_s F_y + \tau'\alpha_1\phi_c A_c f_c'}{(1+\lambda^{2n})^{\frac{1}{n}}} \quad \text{with} \quad \lambda = \sqrt{\frac{C_p}{C_{ec}}} \quad \text{and} \quad C_{ec} = \frac{\pi^2 EI_e}{(KL)^2}$$

where A_s and A_c = cross-sectional area of steel and concrete; ϕ and ϕ_c = resistance factor for steel and concrete (= 0.9 and 0.65, respectively); τ = confinement reduction factor for steel (= 1.0 for concrete-filled RHS); τ' = confinement enhancement factor for concrete (= 1.0, again, for concrete-filled RHS); α_1 = ratio of average stress in rectangular stress block to f_c' (= 0.85 - 0.0015f_c' ≥ 0.73); n = column curve parameter (= 1.80); λ = non-dimensional slenderness parameter; C_p = C_{rc} computed with ϕ = ϕ_c = 1.0 and λ = 0; and EI_e = effective elastic flexural stiffness of the composite column, taken as:

$$[3]\quad EI_e = EI_s + \frac{0.6E_c I_c}{1+C_{fs}/C_f}$$

where I_s and I_c = moment of inertia of the steel and concrete areas, respectively, as computed with respect to the centre of gravity of the cross-section; E = modulus of elasticity of steel; E_c = modulus of elasticity of concrete (found in CSA S16:19 Clause 3); C_{fs} = sustained axial load on the column; and C_f = total axial load on the column.

M_{rc} in Eq. [1] is taken as:

[4] $M_{rc} = C_r e + C_r' e'$ with

[5] $C_r = \dfrac{\phi A_s F_y - C_r'}{2}$ and $C_r' = 1.18\alpha_1\phi_c a(b-2t)f_c'$

[6] $C_r + C_r' = T_r = \phi A_{st} F_y$

where C_r = compressive resistance of steel above the neutral axis (NA); C_r' = compressive resistance of concrete above the NA (over the depth of the concrete compression zone, a); e = lever arm between C_r and T_r; T_r = tensile resistance of steel below the NA (with an area of A_{st}); and e' = lever arm between C_r' and T_r (Fig. 1).

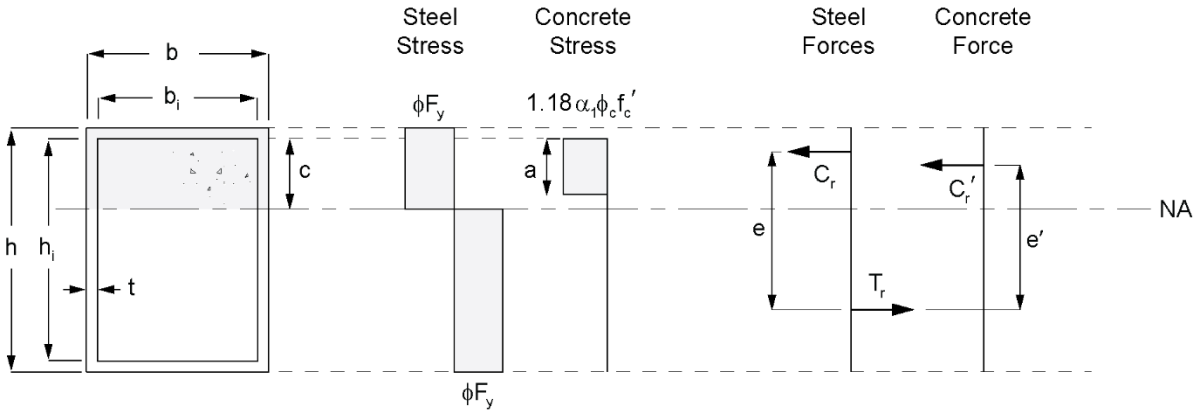

Figure 1: Stress and force diagrams for concrete-filled RHS, simplified to a box section (CSA S16:19)

In the 2009 (CSA 2009) and later editions of CSA S19, the depth of the concrete compression zone, a, relative to the depth of the neutral axis (c, in Fig. 1) was no longer specified. The value of c, however, is determined through the equilibrium of resistances to satisfy Eq. [6].

The coefficient β in Eq. [1] is taken as:

[7] $\beta = \dfrac{C_{rco} - C_{rcm}}{C_{rco}}$

where $C_{rco} = C_{rc}$ calculated with λ = 0 and $C_{rcm} = 1.18\alpha_1\phi_c A_c f_c'$.

It is important to note that in the 2019 edition of the standard (CSA 2019a), changes were made to the β values for unfilled HSS beam-columns in Clauses 13.8.3 and 13.8.4. The rationale for the new values chosen was based on designing the members for plastic behaviour (Essa and Kennedy 2000; Pillai 1974).

2.2 Tousignant and Packer (2022a,b)

The study by Tousignant and Packer (2022a,b) resulted in several proposed changes to CSA S16 Clause 18.2 that cover its scope (i.e., material limitations), the classification of cross sections, and provisions for compressive resistance, bending resistance, and axial compression plus bending.

Tousignant and Packer (2022a) recommended to adopt rounded ranges of 20 MPa ≤ f_c' ≤ 70 MPa for normal-weight concrete and 20 MPa ≤ f_c' ≤ 40 MPa for light-weight concrete in CSA S16. Although the former limit is slightly more restrictive than the current limit in CSA S16 for concentrically loaded columns (f_c' ≤ 70 MPa versus f_c' ≤ 80 MPa), the validated wider range of application for beam-columns is valuable considering that nearly all columns, in practice, are subjected to combined loading.

Tousignant and Packer (2022a) also recommended to replace the current b_{el}/t limit(s) for plastic design in CSA S16 Clause 18.2.1 (see Section 2.1) with the proposed limits in Table 1 of this paper. Despite being more restrictive again (in some cases), these limits are met by nearly all RHS in the CISC Handbook (CISC 2021).

A modification to the C_{rc} equation (Eq. [2]) was also proposed – to cater to the use of longitudinal steel reinforcing bars; i.e.:

$$[8]\ C_{rc} = \frac{\tau\phi A_s F_y + \tau'\alpha_1\phi_c A_c f_c' + \phi_r A_r F_{yr}}{(1+\lambda^{2n})^{\frac{1}{n}}}$$

where A_r = cross-sectional area of longitudinal reinforcement and ϕ_r = resistance factor for steel reinforcing bars. A new lower limit of 0.75 for α_1 was proposed as a consequence of adopting the upper limit of f_c' = 70 MPa discussed previously.

For consistency, it was also recommended that the expression for EI_e (Eq. [3]) be modified to:

$$[9]\ EI_e = EI_s + \frac{0.6E_cI_c}{1+C_{fs}/C_f} + EI_r$$

where I_r = moment of inertia of the reinforcing bar areas, as computed with respect to the centre of gravity of the cross-section.

Tousignant and Packer (2022b) proposed a modification to the equation for M_{rc} in CSA S16 (Eq. [4]) which aimed to make it clearer, as well as to provide for the use of longitudinal steel reinforcing bars; i.e.:

$$[10]\ M_{rc} = Z\phi F_y - 2t(\frac{h_i}{2}-a)^2\phi F_y + \frac{Z_c}{2}\phi_c f_c - \frac{b_i}{2}\left(\frac{h_i}{2}-a\right)^2\phi_c f_c + M_{rr}$$

where $f_c = 1.18\alpha_1 f_c'$; Z = plastic modulus of the steel section alone; and h_i = d-2t (where d = overall depth of hollow section). The depth of the concrete compression zone, a, was also explicitly defined:

$$[11]\ a = \frac{h_i}{2} - \frac{\left(A_g - A_s\right)\phi_c f_c - 2\phi_r F_{yr}\left(A_{src} + A_{srb} - A_{srt}\left(1-\phi_c f_c/\phi_r F_{yr}\right)\right)}{8t\phi F_y + 2b_i\phi_c f_c}$$

where A_g = gross cross-sectional area of composite section; A_{srt}, A_{src} and A_{srb} = area of reinforcing bars in the top, central, and bottom region, respectively, where only the top region is located above the neutral axis; and Z_c = plastic modulus of the area inside the HSS (concrete plus reinforcing bars), taken as:

$$[12]\ Z_c = \frac{b_i h_i^2}{4} - 0.429r_i^2 h_i + 0.192r_i^3$$

where b_i = b – 2t (b = overall width of hollow section); r_i = t; and:

$$[13]\ M_{rr} = \phi_r F_{yr}\left[A_{srt}\left(a-d_c\right)\left(1-\phi_c f_c/\phi_r F_{yr}\right) + A_{src}\left(\frac{h_i}{2}-a\right) + A_{srb}\left(h_i-a-d_c\right)\right]$$

where d_c = distance from the inside face of the RHS to the centre of the closest adjacent reinforcing bar (Fig. 2). The term M_{rr} reflects the incremental contribution to the moment resistance gained by adding steel reinforcing bars.

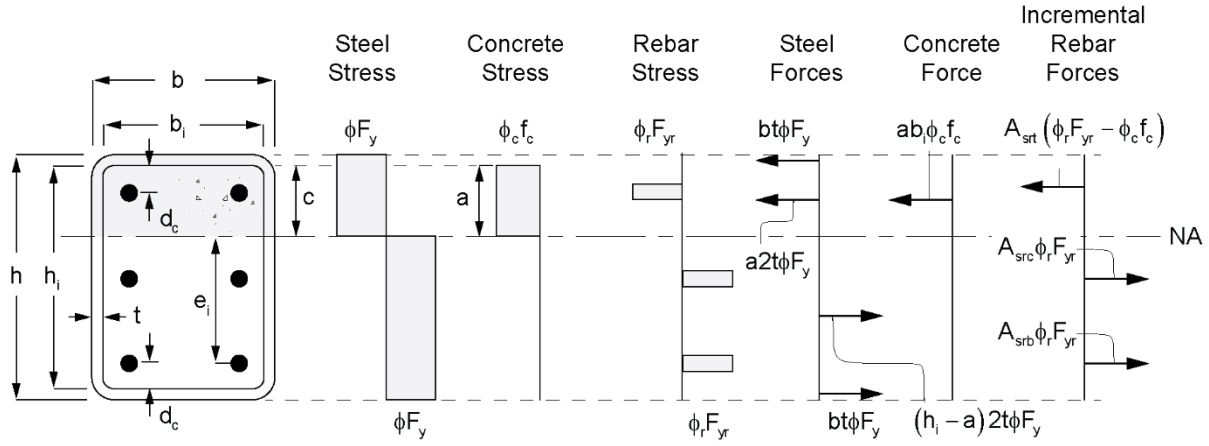

Figure 2: Stress and approximate force diagrams for concrete-filled RHS (proposed)

With respect to beam-columns, Tousignant and Packer (2022b) made several recommendations for consistency. In addition to using the previously discussed C_{rc} and M_{rc} equations (Eqs. [8] and [10], respectively) in Eq. [1], subject to the proposed f_c' and b_{el}/t limits (20 MPa ≤ f_c' ≤ 70 MPa for normal-weight concrete, and Table 1, respectively), they proposed two possible approaches to determine β:

1. Approach (i): using Eq. [7]; and
2. Approach (ii): using "β = 0.85 for square and circular hollow structural sections, and 1.0 for all other hollow structural sections".

Approach (i) was shown to give similar statistics to the existing CSA S16 method, and Approach (ii) was believed to be more conservative. Approach (ii) is in accord with the changes made for unfilled HSS beam-columns in Clauses 13.8.3 and 13.8.4 of CSA S16:19 (CSA 2019a) (see Section 2.1).

3 SCOPE OF ANALYSIS

Herein, the two approaches proposed by proposed by Tousignant and Packer (2022b) for design of concrete-filled RHS beam-columns [Approaches (i) and (ii), above] are evaluated by using MCS to simulate various design scenarios for characteristic members, without reinforcement, over a range of live-to-dead load (L/D) ratios. Reliability indices (i.e., β^+-values) are then obtained and compared to the target value of $\beta^+ = 3.0$ spelled out in Annex B of CSA S16:19 (CSA 2019a).

The reliability indices (β^+) determined herein are based on comparisons of the member resistance (R) and load effect (S) distributions, assuming perfect design (see Section 5.1), whereby the safety margin (G) is given by Eq. [14]:

$$[14]\quad G = \ln(R) - \ln(S)$$

and, hence, a failure event occurs when G < 0.

The probabilistic method used by the Authors relates the probability of failure (i.e., the probability that G < 0) to the mean and standard deviation of G (G_m and σ_G, respectively) using a safety/reliability index (β^+), defined as (Ravindra and Galambos 1978):

[15] $\beta^+ = \frac{G_m}{\sigma_G}$

β^+ can be viewed simply as the number of standard deviations between G_m and the failure condition, for which targets are given in design codes (e.g., CSA 2019a, AISC 2016).

To account for uncertainty in design, R and S are modelled herein as random variables with probability distributions obtained by randomly sampling from the resistance and load effect parameter distributions in Tables 2 and 3.

Table 2: Bias coefficients and COVs for resistance parameters (excluding the professional factors)

Parameter	δ	V	Reference
F_y	1.178	0.086	Xi and Packer (2021)
f_c'	1.270	0.122	Bartlett (2007)
E	1.00	0.019	Kennedy and Gad Aly (1980)
b or h	1.00	0.002	Kennedy and Gad Aly (1980)
t	0.975	0.025	Kennedy and Gad Aly (1980)

Table 3: Bias coefficients and COVs for load effect parameters

Parameter	δ	V	Reference
Live load	0.78	0.32	Schmidt and Bartlett (2002)
Dead load	1.05	0.10	Schmidt and Bartlett (2002)

For each design scenario, a possible resistance and load effect are determined, and this process is repeated 1×10^6 times to approximate the distributions of R and S (from which G, G_m, σ_G and β^+ can then be determined). The basic random variables in Tables 2 and 3 were taken from the literature and are assumed to be log-normally distributed in general accordance with CSA S408-11 (CSA 2011). The symbols δ and V in Tables 2 and 3 denote the bias coefficients (i.e., the means of actual-to-nominal values) and corresponding coefficients of variation (COVs), respectively.

The bias coefficient (δ) and V for F_y in Table 2 were taken from Xi and Packer (2021) which, in turn, came from the database of Liu (2016). The values for f_c' are in accord with those used by Bartlett (2007) which, in turn, are based on Bartlett and MacGregor (1996). Since both F_y and f_c' reflect minimum specified strengths in CSA standards (CSA 2019a,b), their distributions were truncated to limit the selection of bias coefficients (for F_y and f_c') to a minimum of 1.0. The bias coefficients and COVs for E, b, h and t in Table 2 were obtained from Kennedy and Gad Aly (1980).

The additional parameters required to calculate the resistance of concrete-filled RHS beam-columns (e.g., E_c, A_s, A_c, I_s, I_c) were calculated as required from the values of f_c', b, h, and t obtained after randomly sampling from the above distributions. All other variables were assumed to be deterministic, including the outside RHS corner radius (r = 2t), concrete density (ρ_c = 2400 kg/m^2), and effective length (KL). The bias coefficients and COVs for load effects in Table 3 were obtained from Schmidt and Bartlett (2002).

In addition to the above, the probability distribution of R is a function of the so-called “professional factor”, which accounts for imperfect nominal resistance design equation(s). The δ and V values for the professional factor(s) used herein were derived from a large database of experiments on concrete-filled RHS column and beam-column members (see Section 4).

4 DATABASE OF TESTS

A database of tests was extracted from Thai et al. (2019) and screened to include only specimens that met the proposed new limits of validity (for b_{el}/t and f'_c) discussed in Section 2.2. Further screening was performed to remove experiments with F_y < 300 MPa and F_y > 450 MPa to reflect the range of typical measured HSS yield strengths available in Canada.

For the remaining experiments with loading eccentricity (e) > 0, the nominal predicted compressive strength in the presence of bending (C_n) was calculated for Approaches (i) and (ii) by rearranging Eq. [1] with instances of C_f and M_f replaced by C_n and $C_n \times e$, respectively. It was necessary in calculating C_n to assume that $r = 2t$ and $\rho_c = 2400$ kg/m^2 in accord with above. The bias coefficient(s) for the professional factor was then taken as the average of the actual (experimental) strength (C_a) divided by C_n over all tests. The results (δ and V values) are provided in Table 4, which shows that Approach (ii) produces higher C_a/C_n values, on average, but is less precise than Approach (i).

Table 4: Bias coefficients and COVs for the professional factor(s)

		Approach (i)		Approach (ii)	
	n	δ	V	δ	V
Beam-columns (e > 0 mm)	48	1.17	0.19	1.44	0.24
Columns (e = 0 mm)	181	1.27	0.16	1.27	0.16

Figs. 3a,b compare the ratios of C_a/C_n for beam-column tests from the database with values of e and KL from the corresponding experiments. It can be deduced from these plots that the ratio of C_a/C_n decreases somewhat for both approaches as KL goes up. Nonetheless, both approaches [(i) and (ii)] maintain a reasonable level of accuracy over the full range(s) of each variable.

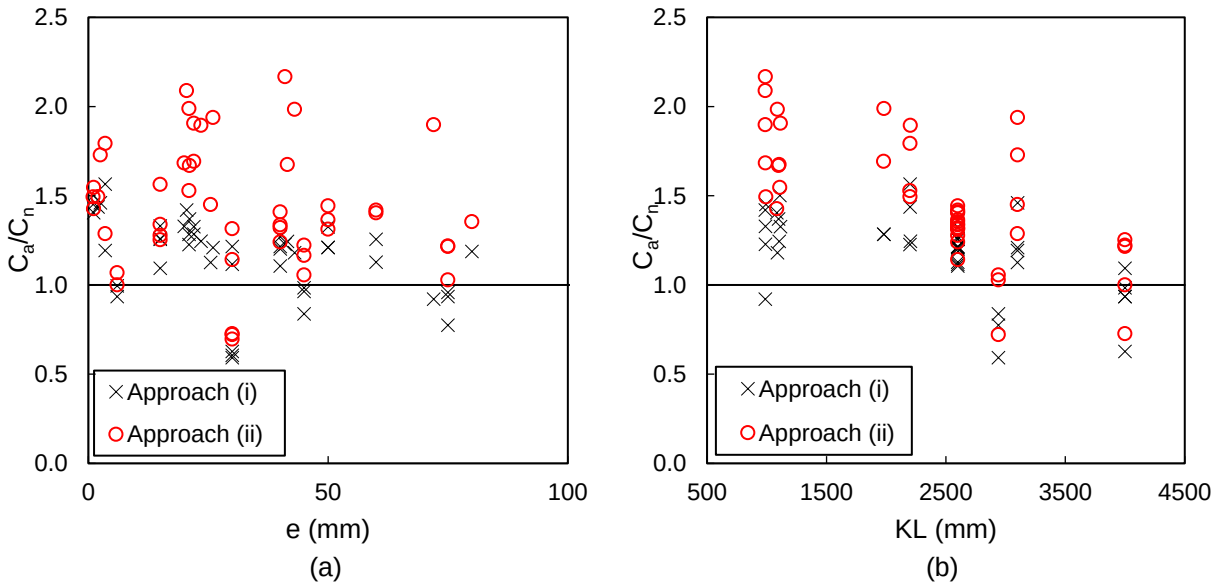

Figure 3: Comparison of 48 concrete-filled RHS beam-column tests to predictions

A similar re-analysis was performed of the Thai et al. (2019) database to determine professional factor statistics for concentrically loaded RHS members with e = 0, which are designed according to Eq. [8]. The values of δ and V determined as part of this study are presented in Table 4, which agree with those given by Tousignant and Packer (2022a).

5 MONTE CARLO SIMULATIONS

5.1 Procedure

A representative set of 10 concrete-filled RHS members was next formulated to cover a range of KL/r and $8 \le b_{el}/t \le 44$. (The maximum b_{el}/t was selected to be within the proposed limits of Table 1). Each member was further analyzed under an axial load applied at three different values of e (= 0, 50, 100 mm) to produce

corresponding ratios of M_f/C_f, as well as for a range of L/D ratios from 0 to 3. In all analyses performed, the nominal strengths of steel and concrete were taken as F_y = 350 MPa and f'_c = 40 MPa, respectively (representative of CSA G40 HSS and regular-strength concrete in Canada) (CSA 2018), and the column length KL was varied to produce KL/r between 40 and 90. Nominal properties of the representative members are summarized in Table 5.

Table 5: Representative members for Monte Carlo Simulation

Member ID	h (mm)	b (mm)	t (mm)	b_{el}/t
1	304.8	304.8	12.70	20
2	304.8	304.8	6.35	44
3	254.0	254.0	12.70	16
4	254.0	254.0	6.35	36
5	203.2	203.2	12.70	12
6	203.2	203.2	6.35	28
7	177.8	177.8	12.70	10
8	177.8	177.8	6.35	24
9	152.4	152.4	12.70	8
10	152.4	152.4	6.35	20

Reliability indices were determined using Eq. [15] for each of the 10 concrete-filled RHS members (times 3 eccentricities, 10 KL/r values, 18 L/D ratios, and two approaches – for a total of 10,800 design scenarios) using the CSA S16 resistance factors of ϕ = 0.9 and ϕ_c = 0.65, and load factors of α_D = 1.25 and α_L = 1.50 when live plus dead load governs (i.e., when L/D ≥ 0.135), and α_D = 1.40 when dead load only governs (i.e., when L/D < 0.135) (NRC 2020).

Hence, for each scenario:

1. The factored resistance of the member was determined using the nominal values of material and geometrical properties discussed above.
2. Random samples were drawn from the probability distributions for resistance parameters in Table 2.
3. The sampled values were multiplied by their nominal counterparts.
4. The nominal member resistance was computed using the corresponding parameter values.
5. A random sample was drawn from the probability distribution(s) for the professional factor(s) in Table 4.
6. The nominal member resistance (Step 4) was multiplied by the professional factor to obtain the final (unfactored) resistance.
7. The nominal dead and live loads required for perfect design (utilization ratio = 1.0) were determined for the governing load case.
8. Random samples were drawn from the probability distributions for load effect parameters in Table 3.
9. The sampled values were multiplied by their nominal counterparts, and the results were summed together, if necessary, to obtain the final (unfactored) load effect.

Steps 1-9 were repeated 1×10^6 times for each for the 10,800 design scenarios, and the resulting distribution(s) of R and S, for each scenario, was used to determine G, G_m, σ_G and β^+. Fig. 4 shows typical plots of R and S distributions obtained by completing 1×10^6 iterations of Steps 1-9 for Member 5 in Table 5, using Approach (i) with e = 50, KL/r = 65.0, and L/D = 1.0. It can be seen, therein, that both distributions are approximately log-normal.

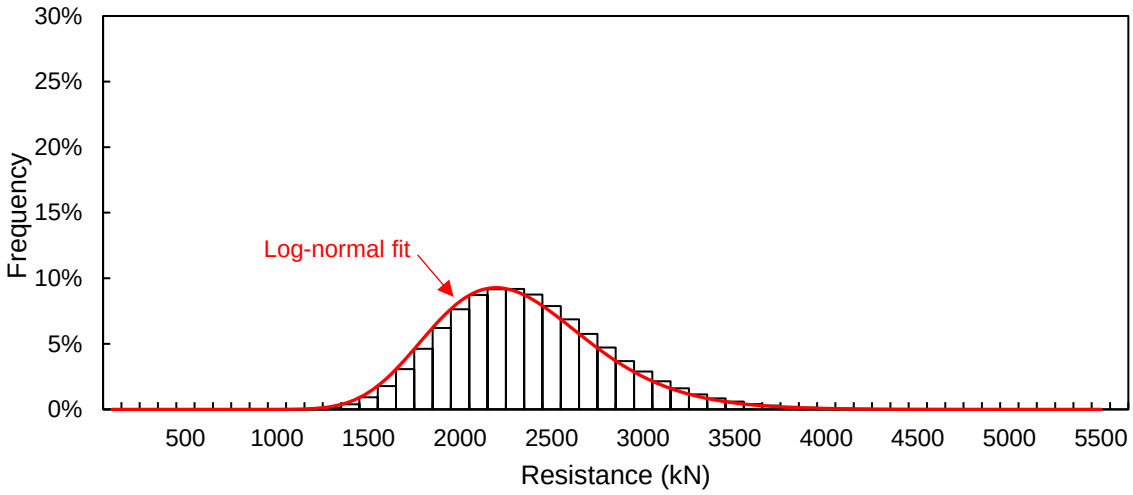

(a) Resistance

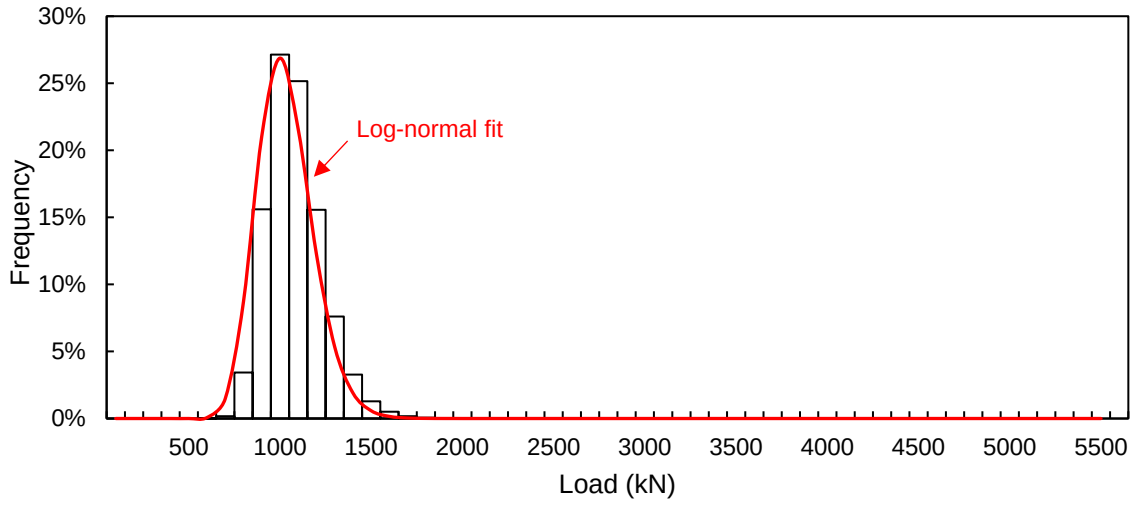

(b) Load effect

Figure 4: Resistance and load effect distributions for Member 5, using Approach (i) with e = 50, KL/r = 65.0, and L/D = 1.0

5.2 Results

The results of the MCS analysis (i.e. plots of β^+ vs. L/D) are shown in Figs. 5a-d. Specifically, Figs. 5a,b illustrate the effect of e on β^+, and Figs. 5c,d illustrate the effect of KL/r. Each of the three curves in Figs. 5a,b and each of the six curves in Figs. 5c,d have been calculated by taking the average β^+ value over all 10 connections at a given L/D ratio.

For Approach (i), when e = 0 mm (Fig. 5a), β^+ ranges from 3.96 to 4.49, and remains well above the target of β^+ = 3.0 in Annex B of CSA S16:19 (CSA 2019a). It is important to note that, for these columns, the professional factor statistics in the last row of Table 4 were used. When e > 0 mm (and hence, when axial load plus moment interaction is considered), Approach (i) yields β^+ values between 3.13 and 3.77, which are again greater than 3.0. There is very little difference in the β^+ values obtained when e = 50 mm and e = 100 mm.

For Approach (ii), when e = 0 mm (Fig. 5b), β^+ ranges from 3.96 to 4.49 [i.e., the same as above – as expected – since the only difference between Approaches (i) and (ii) is the method for calculating β, which is not required for concentrically loaded columns]. When e > 0 mm, on the other hand, β^+ ranges from 2.76 to 3.46. This is slightly lower than for Approach (i) because the increase in bias for Approach (ii) (higher δ, in Table 4) is coupled with a decrease in precision (i.e., higher V). Nonetheless, the resulting ranges of β^+ are still greater than 2.6, on average, for all L/D ratios considered. This value of 2.6 is the minimum reliability index currently expected in North American codes (AISC 2016). Over the practical range of 1 ≤ L/D ≤ 3 for steel members (Schmidt and Bartlett 2002), all β^+ values, for both approaches, exceed 3.0.

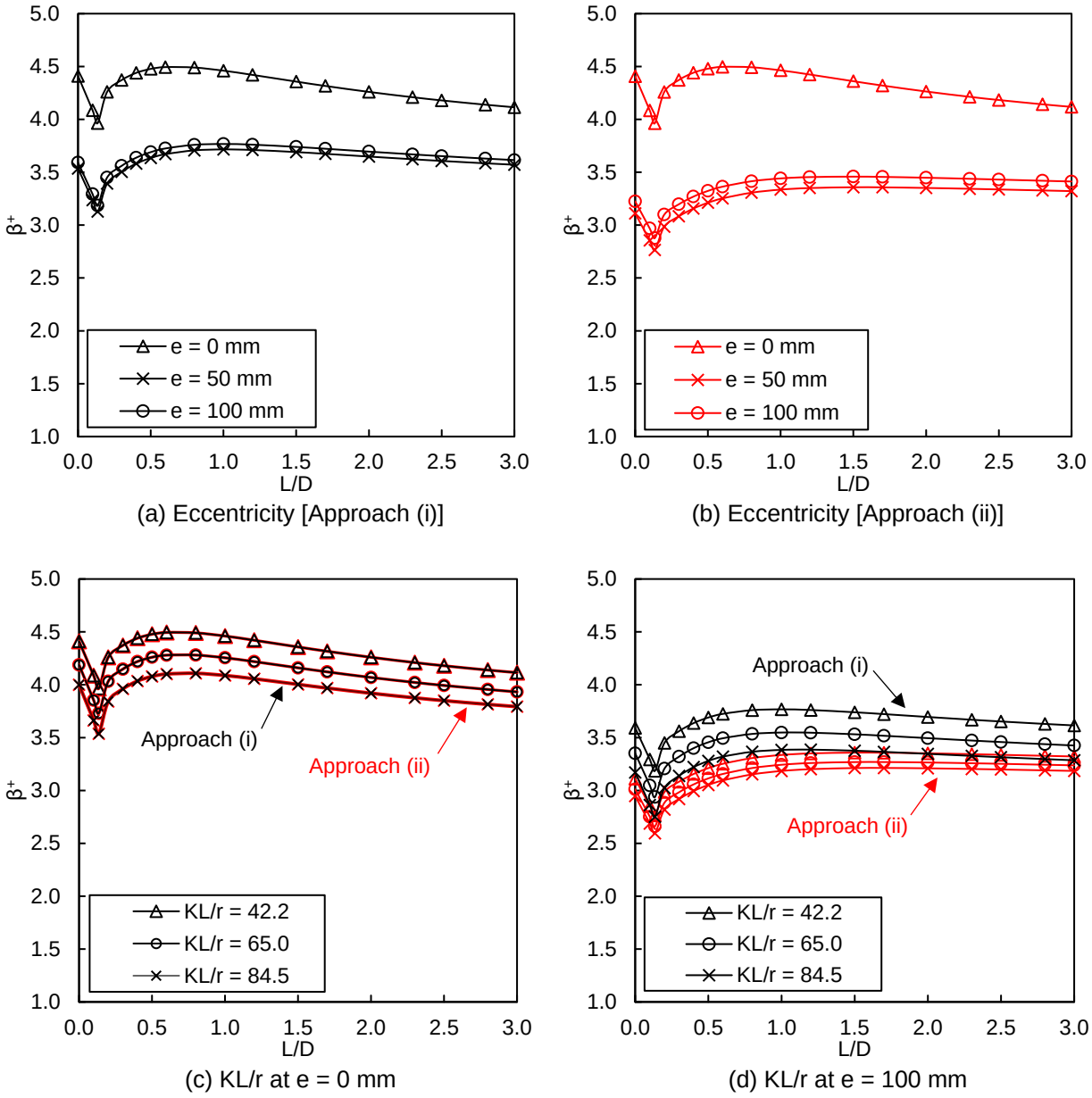

(a) Eccentricity [Approach (i)]

(b) Eccentricity [Approach (ii)]

(c) KL/r at e = 0 mm

(d) KL/r at e = 100 mm

Figure 5: Effects of various parameters on reliability index

Fig. 5c shows (for concentrically loaded columns) that β^+ decreases as KL/r increases in accord with the general trend illustrated in Fig. 3b. Fig. 5d shows a similar trend, but for beam-columns with e = 100 mm.

An "overall" β^+ was computed at each L/D ratio by taking the average β^+ value obtained across all members, eccentricities, and effective lengths. The results [i.e., $3.20 \le \beta^+ \le 3.78$ for Approach (i), and $3.06 \le \beta^+ \le 3.62$ for Approach (ii)] are shown in Fig. 6, which illustrates that β^+ is always greater than 3.0. Based on the above, it can be concluded that the approach(es) proposed by Tousignant and Packer (2022b) for design of concrete-filled RHS beam-columns obtains a level of safety commensurate with CSA S16 (CSA 2019a).

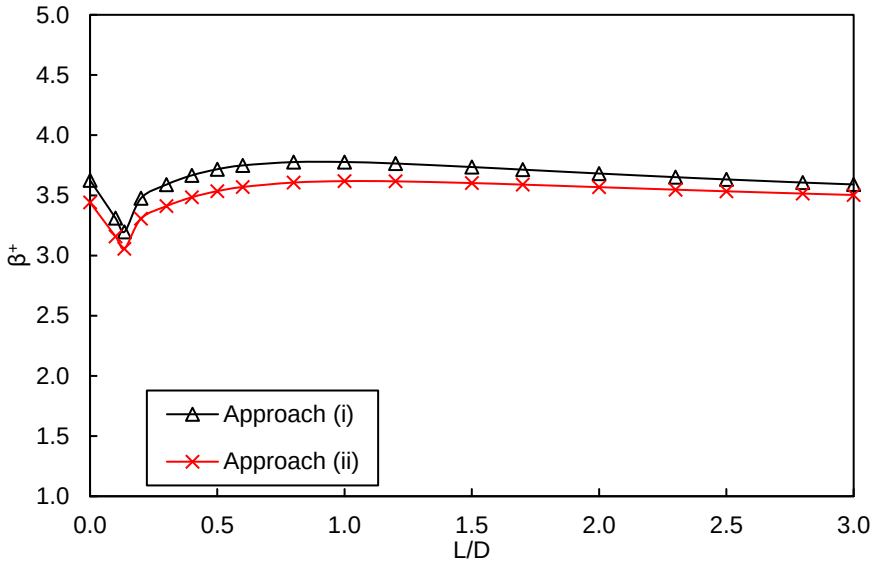

Figure 6: Overall reliability index vs. L/D [both approaches]

6 CONCLUSIONS

Reliability indices were determined for 10 concrete-filled RHS beam-column members over a range of KL/r and $8 \le b_{el}/t \le 44$. Simulations (using MCS) were performed for each member, considering three different loading eccentricities (e = 0, 50 and 100 mm), 10 KL/r values, 18 L/D ratios, and two design approaches [i.e., Approaches (i) and (ii), in Section 2.2, which were proposed by Tousignant and Packer (2022b)]. In total, 10,800 design scenarios were covered, and 10.8×10^9 simulations were performed.

The following conclusions can be made from the results:

- For Approach (i), β^+ ranges from 3.20 – 3.78, on average, with is greater than the target value of $\beta^+ = 3.0$ (CSA 2019). For some scenarios (i.e., some columns, with some values of e and KL/r), β^+ falls below 3.0, but remains above 2.6, which is the minimum value expected in North American codes (AISC 2016);
- For Approach (ii), β^+ ranges from 3.06 – 3.62 on average, which is – again – greater than the target value of 3.0. For some scenarios, β^+ falls (again) below 3.0, but remains above 2.6.
- When $1 \le L/D \le 3$ is considered, which is the common range for steel members, both approaches [(i) and (ii)] produce $\beta^+ \ge 3.0$ across all scenarios considered.

The findings of this research provide evidence to support the use of either approach [(i) or (ii)] for the design of concrete-filled RHS beam-columns within the above parameter ranges in CSA S16.

Acknowledgements

Financial support for this research was provided by the Natural Sciences and Engineering Research Council of Canada (NSERC).

References

AISC. 2016. *Specification for structural steel buildings*. AISC 360-16, American Institute of Steel Construction, Chicago, IL, USA.

Bartlett, F.M. and MacGregor, J.G. 1996. Statistical analysis of the compressive strength of concrete in structures. *ACI Materials Journal* **93**(2): 158-168.

Bartlett, F.M. 2007. Canadian Standards Association standard A23.3-04 resistance factor for concrete in compression. *Canadian Journal of Civil Engineering* **34**: 1029-1037.

CISC. 2021. *Handbook of steel construction, 12th ed.* Canadian Institute of Steel Construction, Toronto, ON, Canada.

CSA. 2001. *Limit states design of steel structures*. CAN/CSA S16-01, Canadian Standards Association, Toronto, ON, Canada.

CSA. 2009. *Design of steel structures*. CSA S16-09, Canadian Standards Association, Toronto, ON, Canada.

CSA. 2018. *General requirements for rolled or welded structural quality steel / Structural quality steel*. CSA G40.20-13/G40.21-13 (R2018), Canadian Standards Association, Toronto, ON, Canada.

CSA. 2019a. *Design of steel structures*. CSA S16:19, Canadian Standards Association, Toronto, ON, Canada.

CSA. 2019b. *Design of concrete structures*. CSA A23.3:19, Canadian Standards Association, Toronto, ON, Canada.

Essa, H.S. and Kennedy, D.J.L. 2000. Proposed provisions for the design of steel beam-columns in S16-2001. *Canadian Journal of Civil Engineering*, **27**: 610-619.

Kennedy, D.J.L. and Gad Aly, M. 1980. Limit states design of steel structures – performance factors. *Canadian Journal of Civil Engineering* **7**: 45-77.

Liu, J. 2016. Updates to expected yield stress and tensile strength ratios for determination of expected member capacity in the 2016 AISC seismic provisions. *Engineering Journal* **53**(4): 215-228.

National Research Council of Canada (NRC). 2020. NBCC 2020 Part 4. *National building code of Canada*. NRC, Ottawa, ON, Canada.

Pillai, U.S. 1974. Beam-columns of hollow structural sections. *Canadian Journal of Civil Engineering*, **1**(2): 194-198.

Ravindra, M. K. and Galambos, T.V. 1978. Load and resistance factor design for steel. *Journal of the Structural Division* **104**(9): 1337-1353.

Schmidt, B.J. & Bartlett, F.M. 2002. Review of resistance factor for steel: Resistance distributions and resistance factor calibration. *Canadian Journal of Civil Engineering* **29**: 109-118.

Thai, S., Thai, H.T., Uy, B. and Ngo, T. 2019. Concrete-filled steel tubular columns: Test database, design, and calibration. *Journal of Constructional Steel Research* **157**: 161-181.

Tousignant, K. and Packer, J.A. 2022a. Concrete-filled hollow structural sections. I: Materials, cross-section classification, and concentrically loaded columns. *Canadian Journal of Civil Engineering* **49**(3): 368-383.

Tousignant, K. and Packer, J.A. 2022b. Concrete-filled hollow structural sections. II: Flexural members, beam columns, tension, and shear. *Canadian Journal of Civil Engineering* **49**(3): 384-400.

Tousignant, K. and Packer, J.A. 2022c. CSA S16:24 – Changes to concrete-filled HSS. *Proceedings, 49th Annual Conference, Canadian Society for Civil Engineering*: STR076-1 – STR076-11.

Xi, Q. and Packer, J.A. 2021. Assessing the probabilistic assumptions behind structural reliability via simulation. *Proceedings, 49th Annual Conference, Canadian Society for Civil Engineering*: STR230-1 – STR230-10.

Zhao, X.L., Packer, J.A., Wang, Y.C. and McCormick, J.P. 2019. *Design guide for concrete-filled hollow section columns under static, impact, blast, seismic and fire loading*. CIDECT Final Report 16H-4/19, Comité International pour le Développement et l'Étude de la Construction Tubulaire, Geneva, Switzerland.